

NEUTRON AND X-RAY SCATTERING IN MATERIALS SCIENCE AND BIOLOGY

*Proceedings of the
International Conference on Neutron and X-ray Scattering 2007*

Serpong and Bandung, Indonesia 23 – 31 July 2007

EDITORS

Abarrul Ikram
Agus Purwanto
Sutiarso
Anne Zulfia
Sunit Hendrana
Zelly Nurachman

AMERICAN
INSTITUTE
OF PHYSICS

AIP CONFERENCE PROCEEDINGS ■ 989

CONTENTS

Committees	ix
Preface	xi
Workshop Program	xiii
Symposium Program	xix

PLENARY LECTURES

Application of X-ray and Neutron Scattering Techniques in Materials Research: Lithium Batteries and Electronic Ceramics (<i>abstract only</i>)	3
A. R. West	
Early Years of Neutron Scattering and Its Manpower Development in Indonesia	4
Marsongkohadi	
Opportunities for Materials Science and Biological Research at the OPAL Research Reactor (<i>abstract only</i>)	10
S. J. Kennedy	
J-PARC and Prospective Neutron Science (<i>abstract only</i>)	11
M. Arai	
Current Status and Future Works of Neutron Scattering Laboratory at BATAN in Serpong	12
A. Ikram	
Magnetic Excitations in Transition-metal Oxides Studied by Inelastic Neutron Scattering (<i>abstract only</i>)	19
M. Braden	
Pulsed Neutron Powder Diffraction for Materials Science (<i>abstract only</i>)	20
T. Kamiyama	
Thermal Stress Behavior of Micro- and Nano-size Aluminum Films	21
T. Hanabusa, M. Nishida, and K. Kasuda	
Neutron Reflectometry as a Surface Probe: A Personal Perspective (<i>abstract only</i>)	28
Z. Tun	
Dynamical Scaling, Fractal Morphology, and Small-angle Scattering	29
S. Mazumder	
Deuterium Labeling and Neutron Scattering for Structural Biology	35
P. Timmins	
Membrane Structure Studies by Means of Small-Angle Neutron Scattering (SANS) (<i>abstract only</i>)	40
R. B. Knott	
Structure and Function of Glucansucrases	41
B. W. Dijkstra and A. Vujičić-Žagar	
Neutron Protein Crystallography: Beyond the Folding Structure	47
N. Niimura	
SANS and DLS Studies of Protein Unfolding in Presence of Urea and Surfactant	53
V. K. Aswal, S. N. Chodankar, J. Kohlbrecher, R. Vavrin, and A. G. Wagh	
Synthesis and X-ray Structural Study on the Complexes of Silver(I) Halide with Tricyclohexylephosphine, Diphenyl-(2,4,6-trimethoxy)phenylphosphine, Phenyl-2,4,6-trimethoxyphenyl phosphine, and Tris(2,4,6-trimethoxy)phenylphosphine (<i>abstract only</i>)	59
Effendy and A. H. White	
Powder Diffraction Studies of Phase Transitions in Manganese Perovskites	60
B. J. Kennedy	
SANS and SAXS Study of Block and Graft Copolymers Containing Natural and Synthetic Rubbers	65
H. Hasegawa	
Small Angle X-ray and Neutron Scattering in the Study of Polymers and Supramolecular Systems (<i>abstract only</i>)	68
X. B. Zeng, F. Liu, F. Xie, G. Ungar, C. Tschierske, and J. E. Macdonald	

The Synthesis and Characterization of Titania Nanotubes Formed at Various Anodisation Time	155
S. Sreekantan, L. M. Hung, Z. Lockman, Z. A. Ahmad, and A. F. M. Noor	
The Influence of Base Concentration on the Surface Particle of Lithium Aluminosilicate System	158
I. M. Nazri, M. A. S. Asliza, and R. Othman	
Effect of Sintering Temperature on the Synthesis of High Purity Cordierite	161
Y. P. Choo, T. Y. Chow, and H. Mohamad	
Synthesis and Characterization of Double Perovskite $Sr_2Mg_{1-x}Mn_xMoO_6$ as Anode Materials in Fuel Cell	164
N. R. Sari, Ismunandar, and B. Prijamboedi	
Phase Compositions of Self Reinforcement $Al_2O_3/CaAl_2O_9$ Composite Using X-ray Diffraction Data and Rietveld Technique	168
D. Asmi, I. M. Low, and B. O'Connor	
Synthesis and Structural Properties of Fe Doped $La_{0.8}Sr_{0.2}Ga_{0.8}Mg_{0.2}O_{3-\delta}$ (LSGM) as Solid Electrolyte for Solid Oxide Fuel Cell	172
Rusmiati, B. Prijamboedi, and Ismunandar	
Size and Correlation Analysis of Fe_3O_4 Nanoparticles in Magnetic Fluids by Small-angle Neutron Scattering	176
S. A. Ani, S. Pratapa, S. Purwaningsih, Triwikantoro, Darminto, E. G. R. Putra, and A. Ikram	
The Use of Rietveld Technique to Study the Phase Composition and Developments of Calcium Aluminate	180
I. Ridwan and D. Asmi	

INSTRUMENTS AND METHODS

Improvements in the Image Quality of Neutron Radiograms of NUR Neutron Radiography Facility by Using Several Exposure Techniques	187
T. Zergoug, A. Nedjar, M. Y. Mokeddem, and L. Mammou	
Performance of SMARTer at Very Low Scattering Vector q-Range Revealed by Monodisperse Nanoparticles	190
E. G. R. Putra, A. Ikram, Bharoto, E. Santoso, and Sairun	
Monochromatic Neutron Tomography Using 1-D PSD Detector at Low Flux Research Reactor	194
N. A. Ashari, J. M. Saleh, M. Z. Abdullah, A. A. Mohamed, A. Azman, and R. Jamro	
Design of the Mechanical Parts for the Neutron Guide System at HANARO	198
J. W. Shin, Y. G. Cho, S. J. Cho, and J. S. Ryu	
Neutron Radiographic Inspection of Industrial Components Using Kamini Neutron Source Facility	202
N. Raghu, V. Anandaraj, K. V. Kasiviswanathan, and P. Kalyanasundaram	

MODELING AND SIMULATIONS

Dynamical Temperature Study for Spin-Crossover	209
W. B. Nurdin and K. D. Schotte	
Genetic Algorithm Application in Solving Crystallographic Phase Problem	214
I. Abdurahman and A. Purwanto	

MATERIALS CHEMISTRY

Structure of Biologically Active Organotin(IV) Dithiocarbamates	221
Y. Farina, M. Sanuddin, and B. M. Yamin	
Study of Mg-doped GaN Thin Films Grown on c-Plane Sapphire Substrate by Plasma Assisted Metalorganic Chemical Vapor Deposition Method	224
A. Subagio, H. Sutanto, E. Supriyanto, M. Budiman, P. Arifin, Sukirno, and M. Barmawi	

Committees

International Advisory Board Members

Dr. A. Aziz Bin Mohamed	MNA, Malaysia
Prof. A. Furrer	ETH Zurich & PSI, Switzerland
Dr. A. J. Hurd	LANSCCE, USA
Prof. Bohari	UKM, Malaysia
Dr. C. J. Carlile	ILL, France
Prof. D. Chen	CIAE, China
Dr. J. Mesot	PSI, Switzerland
Dr. J. Root	Chalk River Laboratories, Canada
Prof. K. Mortensen	Risø National Laboratory, Denmark
Prof. M. Arai	JAEA, Japan
Prof. M. Shibayama	University of Tokyo, Japan
Dr. P. S. Goyal	IUC-DAEF, BARC, India
Dr. T. E. Mason	ORNL, USA
Dr. Y. Morii	JAEA, Japan

National Advisory Board Members

Dr. H. Hastowo	National Nuclear Energy Agency (BATAN)
Dr. S. Soentono	National Nuclear Energy Agency (BATAN)
Dr. P. Anggraita	National Nuclear Energy Agency (BATAN)
Dr. Ridwan	National Nuclear Energy Agency (BATAN)
Dr. A. Ikram	National Nuclear Energy Agency (BATAN)
Dr. A. Purwanto	National Nuclear Energy Agency (BATAN)
Dr. E. Giri Rachman Putra	National Nuclear Energy Agency (BATAN)
Prof. Dr. Marsongkohadi	Bandung Insitute of Technology (ITB)
Dr. Ismunandar	Bandung Insitute of Technology (ITB)
Dr. Z. Nurachman	Bandung Insitute of Technology (ITB)
Prof. Dr. Effendy	State University of Malang (UM)
Prof. Dr. A. K. Prodjosantoso	State University of Yogyakarta (UNY)
Dr. Kgs. Dahlan	Bogor Agricultural University (IPB)
Dr. M. Hikam	University of Indonesia (UI)
Dr. I N. Jujur	Indonesia Agency for Assessment and Application of Technology (BPPT)
Dr. Soetijoso	Padjadjaran University (UNPAD)

PARTICIPANT CONTRIBUTIONS

ALLOYS

Uniform Corrosion of Zirconium Alloy 4 under Isothermal Oxidation at High Temperature	73
D. H. Prajitno	
Degradation of Aluminide Coatings in Fe-Al-Cr Alloy on the Isothermal Oxidation	77
L. Juwita, D. H. Prajitno, J. W. Soedarsono, and A. Manaf	
Oxidation of Ni and Ni-5%W	81
Z. Lockman, M. H. Jamaluddin, and R. Nast	
Texture and Structure Analysis of Aluminum A-1050 Using Neutron Diffraction Technique	85
T. H. Priyanto, N. Suparno, Setiawan, and M. R. Muslih	
The Effect of Sintering Soaking Time on Microstructure and Properties of $\text{CaCu}_3\text{Mn}_4\text{O}_{12}$ System	89
A. R. M. Warikh, A. Z. A. Zahirani, S. D. Hutagalung, and A. Z. Ahmad	
Internal Stress Distribution Measurement of TIG Welded SUS304 Samples Using Neutron Diffraction Technique	92
M. R. Muslih, I. Sumirat, Sairun, and Purwanta	
Residual Stress Estimation of Ti Casting Alloy by X-ray Single Crystal Measurement Method	96
A. Shiro, M. Nishida, and T. Jing	
Residual Stress Measurement of Titanium Casting Alloy by Neutron Diffraction	101
M. Nishida, T. Jing, M. R. Muslih, and T. Hanabusa	

BIOLOGY

Structural Studies of Protein-surfactant Complexes	107
S. N. Chodankar, V. K. Aswal, and A. G. Wagh	
X-ray Powder Diffraction (XRD) Studies on Kenaf Dust Filled Chitosan Bio-composites	111
M. M. Julkapli and M. M. Akil	

CERAMICS

Ferroelectric Properties of $\text{Ba}_2\text{Bi}_4\text{Ti}_5\text{O}_{18}$ Doped with Pb^{2+}, Al^{3+}, Ga^{3+}, In^{3+}, Ta^{5+} Aurivillius Phases	117
A. Rosyidah, D. Onggo, Khairurrijal, and Ismunandar	
Electrical Characteristics of NTC Thermistor Ceramics Made of Mechanically Activated Fe_2O_3 Powder Derived from Yarosite	122
D. G. Syarif and A. Ramelan	
The Effect of SiO_2 Addition on the Characteristics of CuFe_2O_4 Ceramics for NTC Thermistor	126
Wiendartun and D. G. Syarif	
Fractal Studies on Titanium-Silica Aerogels Using SMARTer	130
E. G. R. Putra, A. Ikram, Bharoto, E. Santoso, T. C. Fang, N. Ibrahim, and A. A. Mohamed	
Microstructural and Optical Properties of $\text{Al}_x\text{Ga}_{1-x}\text{N}/\text{GaN}$ Heterostructure Thin Films Grown on Si(111) Substrate by Plasma Assisted Metalorganic Chemical Vapor Deposition Method	134
H. Sutanto, A. Subagio, E. Supriyanto, P. Arifin, M. Budiman, Sukirno, and M. Barmawi	
Dislocations in P-MBE Grown ZnO Layers Characterized by HRXRD and TEM	138
A. Setiawan, I. Hamidah, S. Maryanto, S. Aisyah, and T. Yao	
Fabrication of TiO_2 Thick Film for Photocatalyst from Commercial TiO_2 Powder	143
S. F. Asteti and D. G. Syarif	
Structure and Morphology of Neodymium-doped Cerium Oxide Solid Solution Prepared by a Combined Simple Polymer Heating and D.C.-Magnetron Sputtering Method	147
I. Nurhasanah, M. Abdullah, and Khairurrijal	
The Influence of a Cu-doped on the Structure of $\text{La}_{0.5}\text{Ca}_{0.5}\text{Mn}_{1-x}\text{Cu}_x\text{O}_2$ ($0 < x < 0.2$)	151
Y. E. Gunanto, B. Kurniawan, A. Purwanto, and W. A. Ardhi	

Characterization of a Water-based Surfactant Stabilized Ferrofluid by Different Scattering Techniques	228
V. K. Aswal, S. N. Chodankar, P. U. Sastry, P. A. Hassan, and R. V. Upadhyay	
The Electronic Structure of Wurtzite MnS	233
O. M. Özkendir, A. T. Tüzemen, and Y. Ufuktepe	
Effect of Co-doping on Microstructural, Crystal Structure and Optical Properties of $Ti_{1-x}Co_xO_2$ Thin Films Deposited on Si Substrate by MOCVD Method	237
E. Supriyanto, H. Sutanto, A. Subagio, H. Saragih, M. Budiman, P. Arifin, Sukirno, and M. Barmawi	
Synthesis and Characterization of In-situ Copper-Niobium Carbide Composite	241
H. Zuhailawati, R. Othman, D. L. Biu, and M. Umemoto	
Mechanical Alloying of Mg_2Ni Hydrogen Storage Alloy	245
A. A. Mohamad	
Zircon Supported Copper Catalysts for the Steam Reforming of Methanol	248
M. Widiastri, Fendy, and I. N. Marsih	

POLYMERS AND COLLOIDS

Preparation of Self-assembly Mesoporous TiO_2 Using Block Copolymer Pluronic PE6200 Template	255
W. Septina, B. Yulianto, and Nugraha	
SANS Study of Micellar Structures on Oil Solubilization	259
J. V. Joshi, V. K. Aswal, and P. S. Goyal	
Polyblends of Poly(vinyl alcohol) and Poly(ϵ-caprolactone) and Their Properties	263
I. M. Arcana and L. Alio	
Physical Identification of Binary System of Gliclazide-hydrophilic Polymers Using X-ray Diffraction	268
H. Rachmawati, Yatinasari, Faizatun, and S. A. Syarie	
Effect of Varying Additives on Aqueous Solution of PEO-PPO-PEO Tri-block Copolymer	273
E. G. R. Putra, A. Ikram, and V. K. Aswal	
Sponsors	277
Author Index	279

Organising Committees

Chairman(s)	Dr. E. Giri Rachman Putra Dr. Ismunandar	BATAN ITB
Secretaries	Dr. Sutiarmo Dr. Z. Nurachman	BATAN ITB
Treasurer(s)	Ms. A. Insani Dr. E. Sustini	BATAN ITB
Workshop Coordinator	Dr. A. Ikram	BATAN
Symposium Coordinator	Dr. A. Nugroho	ITB
Poster & Exhibitions	Dr. I N. Marsih Dr. F. Haryanto	ITB ITB
Publication, Documentation & Proceeding	Dr. A. Fajar Dr. B. Prijamboedi	BATAN ITB
Secretariat	Mr. Bharoto Dr. I. Mulyani	BATAN ITB

Size and Correlation Analysis of Fe₃O₄ Nanoparticles in Magnetic Fluids by Small-Angle Neutron Scattering

S. A. Ani¹, S. Pratapa¹, S. Purwaningsih¹, Triwikantoro¹, Darminto¹,
E. Giri Rachman Putra², A. Ikram²

¹ Department of Physics, Faculty of Mathematics and Sciences, Sepuluh Nopember Institute of Technology, Kampus ITS Sukolilo, Surabaya 60111, Indonesia

² Neutron Scattering Laboratory, BATAN, Kawasan Puspiptek Serpong, Tangerang 15314, Indonesia

Abstract. Size and correlation analyses of Fe₃O₄ nanoparticles have been carried out by the measurement of small angle neutron scattering. Particle size of magnetite is analyzed by employing Guinier region approximation in order to obtain gyration radius, which will be used to further determine the average radius of magnetite particles resulting in the value between 17.8 nm and 53.6 nm. Further approximation using a polycore-shell ratio model shows the average particle size of 25 nm with polydispersity of 0.4. The effect of magnetic fluids concentration on the thickness of surfactant layer on the particles surface has not shown a significant change with the value between 6 Å and 8 Å relating to the molar concentration between 0.5 M and 3 M, signifying no correlation among the particles in magnetic fluids.

Keywords: Fe₃O₄ nanoparticle, small angle neutron scattering, magnetic fluids.

PACS: 61.12.Ex, 61.46.Df

INTRODUCTION

Monodisperse magnetic nanoparticles in a self-assembled structure is of technological importance for possible data storage media and is a model system for the study of magnetic interaction in a ferromagnet[1]. The knowledge of magnetic fluids microstructure is very important to understand and control the mechanisms of their stabilization[2]. The neutron scattering methods have been largely used in the last two decades for determination of structural properties of magnetic liquids at microscopic level. Besides, this method can also be developed for examinations of particle size, phenomena of aggregation, magnetic fluid dynamics, particle interaction with surface active agent and magnetic behavior as well[3]. For studies on magnetic phenomena occurring over these length scales of magnetism, small angle neutron scattering (SANS) is exactly appropriate. SANS involves a monochromatic beam of neutrons scattered by the sample and measures the scattered neutrons intensity as a function of the scattering angle. The wave vector transfer extracted from SANS experiment is expressed by

$$Q = \frac{4\pi}{\lambda} \sin 2\theta \quad (1)$$

where 2θ is the scattering angle and λ is the neutron wave length [4]. SANS is a technique that allows us for characterizing structures or objects on the nanometer scale and exploits the big momentum transfer and wavelength reaching out of 3 – 6 Å, which is applicable to observe particle structure in low ordering scattering system being close to the district distance of measurement between 20 – 1250 Å[5].

In this research, we report an analysis concerning the particle size in a low order scattering system in the form of magnetic fluids containing Fe₃O₄ particles using SANS technique. Particle size has been analyzed by Guinier region approximation. Besides, this research also studies the effect of magnetic particle content in magnetic fluids on the layer thickness of surface active agent and their particles correlations.

EXPERIMENT

The Fe₃O₄ magnetic nanoparticles have successfully been synthesized in an aqueous solution by means of the co-precipitation process. We have used iron-sands taken from some rivers in East Java (Sungai Brantas, Kali Madiun and Sungai Regoyo) from which the natural magnetite (Fe₃O₄) can be extracted using a magnetic separator. First, 20 g of natural magnetite was dissolved into 38 mL of 12.06

M HCl at 70 °C under vigorous stirring for 20 minutes. To this solution, 24 mL of 6.5 M NH₄OH was added and the mixture was continuously heated at 70 °C for 20 minutes to induce precipitating process. The precipitate was then washed using de-mineralized water in step by step to gain magnetite nanoparticles using filter papers. The magnetic fluids were finally prepared by adding tetra-methyl ammonium hydroxide to the wet magnetite nanoparticles with varying ratio between surfactant and nanoparticles.

Characterizations of magnetite nanoparticle were conducted by employing X-ray diffractometer (XRD), magnetic force microscope (MFM) and SANS. The structural properties of the as-prepared nanoparticle were analyzed by X-ray powder diffraction with a JEOL JDX 3530 Diffractometer system. The average crystal size was estimated using Rietica internal program. The size distribution of particle has been measured from the enlarged MFM images. Experiments using non-polarized SANS were carried out at Neutron Scattering Laboratory, BATAN, Kawasan Puspipstek Serpong, Indonesia.

The objective of SANS experiment is to determine the differential cross section, which contains all the information concerning with shape, size and interaction of the scattering bodies in the sample [6]. The mathematical expression related to the SANS patterns scattered by the magnetic fluids in conjunction with differential cross section is given by

$$\frac{d\Sigma}{d\Omega}(Q) = n_p (V_p^2) (\Delta\rho)^2 (P(Q))^2 S(Q) \quad (2)$$

where n_p is the number concentration of scattering bodies, V_p is the volume of one scattering body, $\Delta\rho$ is the difference in neutron scattering length density called the contrast for convenience, $P(Q)$ is a function known as the form or shape factor, $S(Q)$ is the interparticle structure factor, and Q is the modulus of the scattering vector [6].

In the dilute particulate system, particles are uniformly dispersed in a matrix. When the particles content is sufficiently small (dilute), the positions of individual particles are apart quite far away from each other to form an uncorrelated system. If the shape of the particles is known, or assumed from the basis of independent information, the intensity of scattering from individual particle can be calculated and compared with the observation. If the particles are of irregular or unknown shape, the data may be analyzed according to the Guinier law to determine the radius of gyration characterizing the size of the particles [7].

The differential scattering cross section for the dilute system is given assuming that the interparticle correlation is small enough and can therefore be

neglected [8]. Using extrapolation for $Q = 0$, since $S(Q)=1$, the cross section is given by

$$\frac{d\Sigma}{d\Omega}(0) = n(V_p^2) (\Delta\rho^2) \quad (3)$$

Guinier [7] has shown that for small values of QR_g , where R_g is the linear dimension of the particle, $P(Q)$ is related to a simple geometrical parameter which is so-called the radius of gyration R_g . Guinier showed further that

$$P(Q) = \exp\left(-\frac{Q^2 R_g^2}{3}\right) \quad (4)$$

scattering function given by equation (4) is called the Guinier law.

$$I(Q) = n(V_p^2) (\Delta\rho^2) \exp\left(-\frac{Q^2 R_g^2}{3}\right) \quad (5)$$

R_g for a particle is defined by

$$R_g = \left[\frac{\int r^2 \rho(r) dr}{\int \rho(r) dr} \right]^{\frac{1}{2}} \quad (6)$$

which is valid typically for $QR_g < 1$. A plot of scattered intensity in the logarithmic scale versus Q^2 results in a straight line for the low Q , and its slope gives the value of R_g .

$$\ln I(Q) = -\frac{1}{3} R_g^2 Q^2 \quad (7)$$

The particle size, no matter whether its shape is geometrically well defined or irregular, can be conveniently characterized by its radius of gyration R_g . The concept of R_g is applicable to particles of any shape, for the purpose of determining the radius of particle [7].

RESULTS AND DISCUSSION

The average crystal size of the Fe₃O₄ analyzed by the powder XRD was around 7 nm, while the particle diameter shown by the MFM image, Fig. 1 varied from 10 to 50 nm. This indicates that Fe₃O₄ particle is secondary particle, meaning that each particle contains several grains. Further, the measured scattering data were converted to the total cross section by subtracting the scattering from an empty cell and ambient background, and by normalizing with the sample transmission and thickness. Fig. 2 shows the one-dimensional average of corrected scattering pattern

from magnetic fluids sample at 0.5M solution concentration and 0.28% of magnetite concentration.

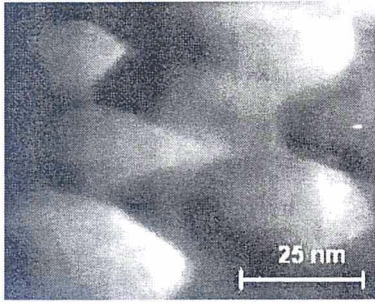


FIGURE 1. MFM images from magnetite particle with average diameter 25 nm

Size and correlation of magnetite particles were analyzed based on the experimental result using two methods. The first method is a fitting program using Guinier region approximation at interval Q -range between 0.8 nm^{-1} and 1.2 nm^{-1} to determine the average particle size. The gradient of $\ln(I)$ to Q^2 plot is applicable to determine radius gyration (R_g) which will be used then to determine the radius of magnetite particle. Gradient at Guinier region is proportional to $^{-1/3} R_g^2$. In Fig. 3 there are three characteristics of particle size for the magnetic fluids with the concentration of 0.5 M and magnetite concentration of 0.28% (Fig. 3). They correspond to the length intervals of 17.8 nm, 29.4 nm, and 53.6 nm. We suppose that the reason may probably be connected with the polydispersity of magnetite particle size in magnetic fluids.

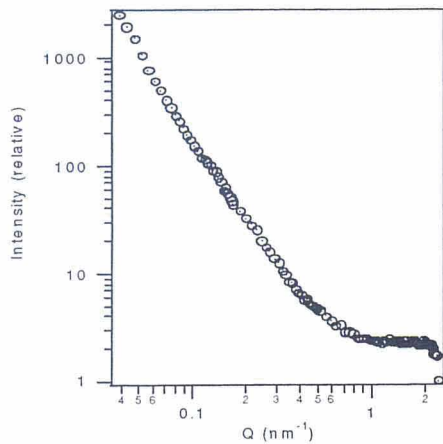


FIGURE 2. Scattering pattern from magnetic fluids with the concentration of 0.5 M and magnetite concentration of 0.28 %.

It is interesting to go further using the approximation of polycore-shell ratio model to determine the polydispersity of magnetite particles. It

has been analyzed in this regards by assuming that the particle is spherical and the fluids contain of magnetite as core, surface active agent as shell and the water as solvent. This curve calculated according to the expected model of polydispersed spheres with scattering length density of magnetite gives result $\rho_c = 6.921 \times 10^{-5} \text{ \AA}^{-2}$. The polydispersity of 0.4 shows that the most particles have average radius of 25 nm, Fig. 4).

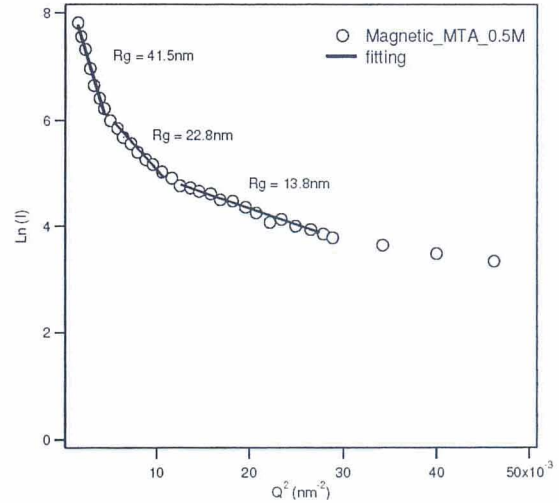


FIGURE 3. Characterize the radius of gyration of the magnetite particle

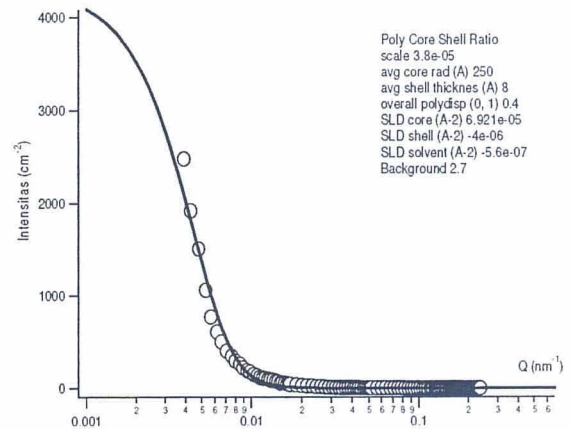


FIGURE 4. Polycore-shell ratio model to determine polydispersity of magnetite particle

The thickness of surfactant shell is the key parameter, which determines the stability of the fluids [11]. It has been shown that in the case of magnetite/tetramethyl ammonium hydroxide/water, the thickness of the surfactant layer will change, when the magnetite concentration is varied. The effect of magnetic fluids concentration on the thickness of

surfactant layer on the particles surface has not significantly been observed. A change with the value between 6 Å and 8 Å corresponds to the molar concentration between 0.5 M and 3 M, signifying no correlation among the particles in magnetic fluids. In the case of the magnetite concentration of 0.28 %, the large penetration between sub-layers of the double surfactant was detected.

TABLE 1. The result of pattern analysis of SANS to determine the thickness of surfactant layer

Concentration of magnetic fluids (M)	volume of magnetite particle Fe_3O_4 (%)	Q (nm^{-1})	Intensity (cm^{-2})	The thickness of surfactant layer (Å)
0.5	0.28	0.112	118.65	8
1	0.55	0.112	193.73	7
2	1.11	0.112	344.18	6
3	1.67	0.112	344.18	6

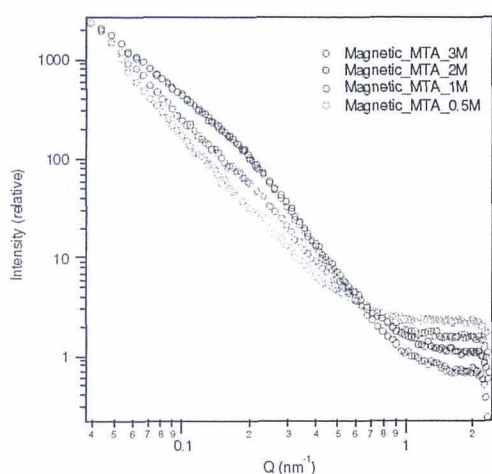


FIGURE 5. Scattering pattern of intensity $I(Q)$ versus Q at different magnetic fluids concentration

The average radius of particle has not been changed significantly with increasing the magnetic concentration. The particle radius ranges at interval between 17.8 nm and 53.6 nm using polycore-shell ratio model with average radius of 25 nm. It shows that there are no correlations of magnetite particle in the concentration range of 0.5 M and 3 M, Fig. 5. A significant decrease in the background of scattering pattern was observed from the sample with increasing magnetite concentration.

CONCLUSIONS

Size and correlation in magnetic fluids structure of magnetite/tetramethyl ammonium hydroxide/water were determined by means of non-polarized SANS. Three characteristics of the average radius of magnetite with the magnetite concentration in the range of 0.28-1.67 %-Volume were obtained and determined using Guinier region approximation and compared with polycore-shell ratio model to result in the thickness of surfactant layer, corresponding to the radius intervals of 17.8 nm, 29.4 nm, and 53.6 nm. We conclude that the reason may be connected with the polydispersity of magnetite particle in the magnetic fluids. The polydispersity of 0.4 shows that the most particles have average radius of 25 nm using polycore-shell ratio model. The effect of magnetic fluids concentration on the thickness of surfactant layer on the particles surface has not been shown significantly, signifying no correlation among the particles in the magnetic fluids.

ACKNOWLEDGMENTS

This work was partially supported by the program of Research Incentive in Nanoscience and Nanotechnology, prepared by the State Ministry of Research and Technology (KMRT), Republic of Indonesia, 2006.

REFERENCES

1. D.F. Farrell, Y. Ijiri, C.V. Kelly, J.A. Borchers, J.J. Rhyne, Y. Ding, S.A. Majetich. *J. Magn. Magn. Mater* **303**, 318-322 (2006).
2. M.V. Avdeev, M. Balasoïu, V. L. Aksenov, V.M. Garamus, J. Kohlbrecher, D. Bica, L.Vekas. *J. Magn. Magn. Mater* **270**, 371-379 (2004).
3. M. Balasoïu, M.V. Avdeev, V. L. Aksenov, V. Ghenescu, M. Ghenescu, Gy. Torok, L. Rosta, D. Bica, L. Vekas, D. Hasegan. *Romanian Rep.Phys.* **56**, 4, 601-607 (2004).
4. V. K. Aswal, P. S. Goyal, *Curr. Sci.* **79**, 7 (2000).
5. J. Kohlbrecher, "Characterization of Nanomagnetic Structures by Polarized Small Angle Neutron Scattering", at <http://kur.web.psi.ch/>
6. S. M. King. *Small Angle Neutron Scattering*. Link fixed Sep 2003.
7. Ryong-Joon Roe, "Methods of X-Ray and Neutron Scattering in Polymer Science", Oxford University Press, Inc., New York, 2000
8. P.S. Goyal, "Small Angle Neutron Scattering", IAEA Workshop on SANS, BARC, Mumbai, India, April 1995.